

# Hawking radiation from acoustic black holes in relativistic heavy ion collisions

Arpan Das<sup>a,b</sup>, Shreyansh S. Dave<sup>c</sup>, Oindrila Ganguly<sup>a,1,\*</sup>, and Ajit M. Srivastava<sup>d</sup>

<sup>a</sup>Physical Research Laboratory, Ahmedabad 380009, India

<sup>b</sup>Institute of Nuclear Physics, Polish Academy of Sciences, PL-31-342 Kraków, Poland

<sup>c</sup>The Institute of Mathematical Sciences, Chennai 600113, India

<sup>d</sup>Institute of Physics, Bhubaneswar 751005, India

---

## Abstract

We propose a new analogue model of gravity - the evolving quark gluon plasma (QGP) produced in relativistic heavy ion collisions. This quark gluon plasma is the “most inviscid” fluid known. Such low kinematic viscosity is believed to reflect strongly correlated nature for QGP in these experiments. Hence, it may provide a good example of a quantum fluid naturally suited to studies of acoustic Hawking radiation. Due to rapid longitudinal expansion, presence of a sonic horizon is also naturally guaranteed here, though, in general, this horizon is not static. Using *Ultra relativistic quantum molecular dynamics* (UrQMD) simulations, we show that, under certain conditions, the longitudinal velocity of the plasma, near the sonic horizon, can become time independent for a short span during the evolution of the system. During this period, we can have a conformally static acoustic metric with a (conformal) Killing horizon coinciding with the apparent horizon. An asymptotic observer will then see a thermal flux of phonons, constituting the Hawking radiation, coming from the horizon. For the relatively low energy collision considered here, where the resulting QCD system is governed by non-relativistic hydrodynamics, we estimate the Hawking temperature to be about 4-5 MeV (with the temperature of the QCD fluid being about 135 MeV). We discuss the experimental signatures of this Hawking radiation in terms of a *thermal* component in the rapidity dependence of the transverse momentum distribution of detected particles. We also discuss extension to ultra-relativistic case which should lead to a higher Hawking temperature, along with the effects of dynamical horizon leading to blue/red shift of the temperature.

---

## 1. Introduction

One of the startling and not classically intuitive characteristics of a black hole is its evaporation. Hawking had shown that black holes *spontaneously* emit thermal radiation, named after him as Hawking radiation, at a temperature  $T_H = 1/8\pi M$  (in natural units),  $M$  being the mass of the black hole [1]. For a stellar mass black hole of mass  $M \approx M_\odot \approx 10^{30} \text{ kg}$ , the Hawking temperature turns out to be  $T_H \approx 10^{-7} \text{ K}$ , which is much less than the temperature of cosmic microwave background radiation. So, at present stage, it is virtually impossible to detect Hawking radiation through astronomical observations.

Hawking radiation is an artefact of the way quantum fields behave in curved spacetime. Interestingly, it so happens that in an inviscid fluid with barotropic equation of state and irrotational bulk velocity, acoustic perturbations in the velocity potential obey an equation which is identical to the Klein Gordon equation satisfied by a mass-

less scalar field in curved spacetime [2]. Thus, the acoustic perturbations perceive an *effective* acoustic spacetime whose geometry is determined by the bulk velocity profile, density and pressure of the fluid. If the fluid flows in such a way that there exists a surface on which at every point the inward normal component of the fluid velocity becomes equal to the speed of sound in the fluid and becomes supersonic beyond it, then all acoustic perturbations originating in the supersonic region are swept inwards by the flowing fluid. This surface acts as a horizon for acoustic perturbations, thus forming an ‘acoustic black hole’ or a ‘dumb hole’. Unruh chose a spherically symmetric, stationary, convergent background flow to construct an analogue of the spacetime outside a Schwarzschild black hole and showed that quantised acoustic perturbations could be emitted from the horizon of such a dumb hole with a thermal spectrum, just like the emission of radiation from a black hole horizon via Hawking radiation [2, 3]. A disconcerting aspect of this remarkable find is that it requires the quantisation of linearised acoustic perturbations in a classical fluid! In reality, to see Hawking radiation in alternate systems, we need a quantum analogue model that can be described in terms of a classical effective background spacetime with some standard relativistic quantum fields living on it [4]. Quantum fluids like superfluid helium, Bose Einstein condensates (BEC), photon fluid etc. are

---

\*Corresponding author

Email addresses: arpan.das@ifj.edu.pl (Arpan Das), shreyanshd@imsc.res.in (Shreyansh S. Dave), oindrila@iisc.ac.in (Oindrila Ganguly), ajit@iopb.res.in (and Ajit M. Srivastava)

<sup>1</sup>Present affiliation: Indian Institute of Science, Bengaluru 560012, India

promising in this regard (for a review, see ref. [4, 5]). In fact, very recently, correlation between Hawking particles and their partners beyond the acoustic horizon of analogue black holes have been observed in a series of experiments using one dimensional flowing atomic condensates [6, 7, 8].

A novel system which is yet to be explored from this perspective is the longitudinally expanding quark gluon plasma (QGP) created in relativistic heavy ion collisions (HIC). Here, two heavy nuclei, moving at speeds close to the speed of light,  $c$ , collide and move through each other. Owing to the extremely high temperature and density produced during collision, a quark gluon plasma is formed. This plasma fills up the space between the two receding nuclei which continue to move away from each other at speeds approaching the speed of light,  $c$ . The velocity of the plasma fluid monotonically increases from zero at the centre of collision (in the centre of mass frame) to a value very close to  $c$  near the receding nuclei. It is then obvious that the fluid velocity becomes supersonic at some surface within the plasma leading to the formation of an acoustic horizon. A very important observation regarding the QGP produced in relativistic heavy-ion collisions at very high energies (e.g. at RHIC and at LHC) is that the produced QGP is the “most inviscid” fluid known with the lowest value of shear viscosity to entropy density ratio,  $\eta/s$ , of all known fluids. This was a very surprising result, as the expectation was that such a QGP system would be close to the ideal gas limit with corresponding large viscosity. Such a low value of kinematic viscosity is believed to reflect the strongly correlated nature of QGP in these experiments and is referred to as sQGP (strongly correlated QGP). Hence, this QGP system may provide a good example of a quantum fluid, fulfilling all the requirements for the presence of acoustic Hawking radiation. Additionally, this gravitational analogy can unravel facets of the plasma that have remained hidden otherwise.

We mention that the actual system we study in this paper is a non-relativistic plasma of nucleons resulting from an Ultra relativistic quantum molecular dynamics (Ur-QMD) simulation of relatively low energy heavy-ion collisions as appropriate for the Beam Energy Scan at RHIC, and for FAIR/NICA energies. For such a system,  $\eta/s$  is expected to be larger, so presence of strong quantum correlations is not so obvious. However, as we will show below in Sect. 3, even here one can argue for the quantum nature of the fluid from the fact that Fermi-Dirac distribution with large chemical potential provides a much better fit of the simulation results than the Maxwell-Boltzmann distribution. Thus, quantum statistics plays an important role here. Before we specialise to such a non-relativistic plasma of nucleons produced in a low energy collision, it is worthwhile to have a general picture of the acoustic black hole for the ultra-relativistic case as appropriate for RHIC and LHC.

For ultra-relativistic collisions, the resulting QGP system is expected to follow Bjorken’s longitudinal boost invariant expansion model during early stages. Here, flow

velocity has only z-component  $v^z$  (along the beam axis), with the scaling law  $v^z = z/t$  as measured in the centre of mass frame.  $t = 0$  corresponds to the instant when the two (highly Lorentz contracted) nuclei overlap. Subsequently, the nuclei go through each other, and while receding away at ultra-relativistic speeds, populate the intermediate region with QGP resulting from interactions of partons in the colliding nuclei. (It has been argued in ref. [9] that acceleration of initial partons in the color glass condensate field during this stage will lead to Hawking-Unruh thermal radiation which can result in rapid thermalisation.) The flow velocity of the plasma exceeds the sound velocity at some location in the region between each receding nucleus and the origin of the centre of mass frame, which becomes the location of the acoustic horizon.

However, it is easily seen that with Bjorken longitudinal scaling expansion,  $v^z = z/t$ , the acoustic horizon is not static, rather it moves away from the centre of collision at the speed of sound. This is not the usual picture of acoustic black hole where horizon is supposed to be static, leading to the standard picture of Hawking radiation. The situation of dynamical horizon for black holes has deep conceptual issues, and has been extensively discussed in the literature (see for example ref. [10] and references therein). Intuitively one may expect that a horizon receding away from the asymptotic observer should lead to red-shifted Hawking radiation while a horizon moving towards the observer will lead to blue shifted radiation. For an acoustic black hole horizon which is moving away with speed of sound (as in Bjorken’s scaling expansion model), one will then expect infinite redshift, making the Hawking radiation unobservable.

However, Bjorken’s scaling expansion model is not strictly valid for the entire plasma region, even for ultra-relativistic case. For large rapidity regions, especially near the receding nuclei, one expects significant deviations from the scaling law due to non-trivial gradients of energy density and pressure. Certainly, for low energy collisions, the scaling law is not valid even in the central regions. In such situations, the velocity of the acoustic horizon may be much smaller than the speed of sound. In fact, as we will see below for simulations with low energy collisions, in certain cases the acoustic horizon may even move towards the asymptotic observer located at the centre, instead of receding away. Additional richness in the motion of acoustic horizon can result from non-trivial dependence of the speed of sound on energy density and pressure. To allow for these different possibilities, one has to consider the issue of Hawking radiation with dynamical horizon. This being a complex issue, we postpone its discussion for future work. In the present work we confine our attention to specific situations in which, due to a balance between the decreasing velocities at a given point due to longitudinal expansion, and acceleration due to non-trivial pressure gradients, one is able to achieve almost static acoustic horizon for few fm duration of time. This becomes a conceptually clean case where the conventional calcula-

tions of Hawking radiation can be employed. This situation is achieved in simulations at relatively low collision energies, and naturally we find the resulting Hawking temperature to also have a small value, about 4 MeV (with the fluid temperature being about 135 MeV). Though, this is a small value, and may be difficult from observational point of view, this case illustrates the existence of this novel phenomenon of Hawking radiation from acoustic black holes in heavy-ion collisions. We expect much higher temperatures for the ultra-relativistic case, along with effects of red/blue shift of the Hawking radiation due to dynamical horizon.

We start with a brief overview of our system in the following section and show how an effective dynamical acoustic metric may be obtained under certain simplifying assumptions. In section 3, we discuss conditions for local thermodynamic equilibrium for plasma with UrQMD simulations and then determine the space and time dependence of its longitudinal velocity. We find a small window of about 2 fm time during which the longitudinal velocity of the plasma becomes almost time independent in the region around the sonic horizon. Confining ourselves to this tiny window, in section 4, we write down the corresponding acoustic metric which is static but for a spacetime dependent conformal factor. We deduce the surface gravity of the (conformal) Killing horizon and the Hawking temperature that an asymptotic observer (located at  $z = 0$  where the fluid velocity is zero) would measure. We discuss the issue of non-trivial conformal factor, and its time dependence, on the Hawking temperature. Finally, in section 5, we discuss observational prospects of acoustic Hawking radiation in this new analogue model of gravity and conclude by pointing out scopes for improvement of this first study, in particular, extension to the relativistic hydrodynamics case and consideration of dynamical horizon. A comment on notation: we use Greek alphabets to denote spatial indices and lowercase Latin alphabets to denote spacetime indices.

## 2. The system

In a relativistic heavy ion collision, two heavy nuclei (like Pb, Au) approach each other at relativistic energies, along a line, collide and pass through each other. Owing to the high energy of collision, a quark gluon plasma (QGP) is formed (or a hadronic plasma, at low energies), after attaining local thermodynamic equilibrium. For ultra-relativistic collisions, the resulting quark gluon plasma (e.g. at RHIC and at LHC) is the most ideal fluid known to exist in nature, with a value of kinematic viscosity ( $\nu = \frac{\eta}{s}$ ,  $\eta$  and  $s$  being the coefficient of shear viscosity and specific entropy of the plasma respectively), lower than any other known material in nature [11]. This is one of the most important, and surprising, results from these experiments and is deduced from the measurements of elliptic flow in non-central collisions [11].

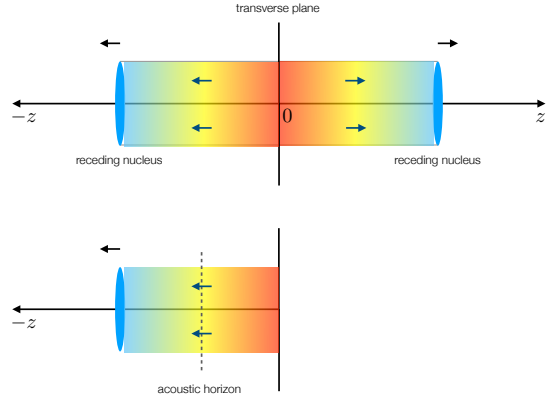


Figure 1: Schematic representation of quark gluon plasma formed by the collision of two heavy (Lorentz contracted) nuclei. For illustration purpose, longitudinal direction is exaggerated. For the time scales relevant, longitudinal dimension of the system is much smaller than the transverse dimension.

The plasma initially acquires only a longitudinal velocity from the colliding nuclei and has zero transverse velocity (transverse to the beam direction). At this point, to visualise the scenario, we introduce a laboratory observer whose frame coincides with the centre of mass (CoM) frame of the colliding nuclei with the  $z$  axis along the longitudinal direction. The time of collision is taken to be  $t = 0$ . Figure 1 schematically represents the situation at a particular instant of time after collision. Initially, the three velocity of the plasma has the form  $v^\alpha(t, x, y, z) = (0, 0, \pm v^z(t, z))$  where the upper and lower signs denote velocities of the plasma in the right ( $z > 0$ ) and left ( $z < 0$ ) half spaces respectively.  $|v^z|$  ranges from zero at  $z = 0$  to almost the speed of light close to the receding nuclei. Let  $\epsilon(t, x, y, z)$  and  $p(t, x, y, z)$  be the energy density and pressure of the plasma respectively, related by a barotropic equation of state (EoS)  $p \propto \epsilon$  [12, 13, 14, 15, 16]. Now, we make three simplifying assumptions to be employed while viewing the system as an analogue model of gravity. Firstly, we assume that the velocities  $v^x, v^y$  can be ignored in comparison to  $v^z$  for the time scales considered here. This is expected for times less than  $\sigma_T/c_s$  [17] where  $\sigma_T$  is the initial transverse size of the resulting plasma (expected to be of order 3 fm for a central Au-Au collision at RHIC energies), and  $c_s$  is the speed of sound. (This is a rough estimate. For a more careful account of the transverse expansion time scale, one should use better estimates, such as using the Blast wave model [18]. We are not able to address such details, this being a preliminary investigation of this kind. Also, in our way of determining equilibrium in a relatively large cell at each value of  $z$ , to some extent, any transverse expansion would already have been accounted for. We can probably safely say that at least within roughly the region of transverse dimensions (about 5 fm) of the cells used for determining equilibrium, one can neglect transverse expansion for the relevant time scales here.) Thus the variables  $\vec{v}, \epsilon, p$  will be functions only of time  $t$

and position along the  $z$  axis. Thus, the velocity field can now simply be written as  $v^\alpha(t, z) = (0, 0, \pm v^z(t, z))$ . The monotonic increase of  $|v^z|$  from zero to values close to the speed of light in each half space ensures that somewhere in each half of the expanding plasma,  $|v^z|$  crosses the sonic value and an acoustic horizon is formed.

The dynamics of the quark gluon plasma should be described by relativistic equations for the conservation of energy and momentum as the plasma velocity takes relativistic values and its equation of state is that for a relativistic fluid. However, as a first approximation towards constructing a new analogue model of gravity, in this work we use non-relativistic hydrodynamics instead. This is not unreasonable, as for the actual QGP system, we will restrict to fluid velocities of order, and less than, the sound speed which will be less than  $1/\sqrt{3}$  (in units of speed of light,  $c$ ). Thus, relativistic corrections will not be very large. For the equation of state part, we are only assuming a barotropic equation of state, so the relativistic aspect of equation of state is not playing a major role here. In fact the UrQMD simulation we have carried out, deals only with hadronic degrees of freedom, and we include only nucleons (protons and neutrons), so our non-relativistic treatment is consistent with that. Under this approximation, the mass density  $\rho(t, z)$  of the plasma becomes relevant in place of the energy density  $\epsilon(t, z)$  and the barotropic condition is  $\rho(p)$ . We consider the stage when thermal equilibrium has been attained (to a good approximation, as discussed below) so that nucleons follow a Fermi Dirac distribution with a large value of the baryon chemical potential, (instead of the Boltzmann velocity distribution which holds for longer times [19]). Thus quantum statistics is relevant, again justifying the quantum nature of the fluid. This observation is very important. Note that we earlier argued that for ultra-relativistic collisions, the very low values of  $\eta/s$ , close to the AdS/CFT limit, suggest presence of strong quantum correlations, justifying the quantum nature of fluid which is of crucial importance for Hawking radiation from the acoustic black hole. However, for the non-relativistic nucleonic plasma resulting from a low energy heavy-ion collision,  $\eta/s$  is larger, so its value cannot be used as an indicator of the presence of strong quantum correlations. However, as we discussed above, the quantum nature of fluid here is manifest from the fact that quantum statistics with the Fermi-Dirac distribution provides a much better fit compared to the Maxwell-Boltzmann distribution.

When talking about the acoustic spacetime, we intend to restrict ourselves to the region  $-\infty < z \leq 0$ . This ensures that the plasma flows towards decreasing values of the longitudinal coordinate  $z$ . The velocity field  $v^\alpha(t, z) = (0, 0, -v^z(t, z))$  is naturally irrotational, thus allowing us to express the velocity  $\vec{v}(t, z)$  in terms of a scalar velocity potential  $\psi(t, z)$  as  $\vec{v} = \vec{\nabla}\psi$ .

With these assumptions in place, the plasma satisfies all the criteria necessary for the construction of an ana-

logue model of gravity. Hence, we can directly write down the effective acoustic metric emerging in this plasma, in coordinates  $(t, x, y, z)$  [3, 20, 21]:

$$ds^2 = \frac{\rho(t, z)}{c_s(t, z)} \left[ - (c_s(t, z)^2 - v^z(t, z)^2) dt^2 + 2v^z(t, z) dt dz + dx^2 + dy^2 + dz^2 \right]. \quad (1)$$

Here,  $c_s(t, z)$  is the speed at which acoustic perturbations propagate in the fluid and is defined by  $c_s^2 = \partial p / \partial \rho$ . Note the relativistic form of the acoustic metric, with speed of light  $c$  replaced by the sound speed  $c_s$ , even though the starting fluid equations are non-relativistic [3]. We mention here that our starting fluid equations are for an ideal fluid with zero viscosity. Acoustic metrics emerge more naturally in fluids with negligible viscosities compared to viscous ones, though a derivation of the same for a relativistic viscous fluid has been given in [22]. Our assumption of inviscid nature of the fluid is reasonable in view of relatively small values of the hadronic phase viscosity [23, 24]. Note that this assumption of zero viscosity is unrelated to our earlier discussions of ultra relativistic collisions where very low values of  $\eta/s$  were related to strong quantum correlations, justifying quantum nature of the fluid.

This metric is qualitatively similar to a time dependent, spherically symmetric metric written in Painlevé-Gullstrand coordinates [20] except that the spatial part in the latter has spherical symmetry while ours has axial symmetry about the longitudinal ( $z$ ) axis. At  $z = 0$ ,  $v^z = 0$  and the above metric reduces to that of a flat spacetime. An apparent horizon or marginally outer trapped surface forms at a value of  $z$  implicitly defined by

$$|v^z(t, z_H)| = c_s(t, z_H). \quad (2)$$

The plasma becomes supersonic in the region  $z < z_H$  and any acoustic perturbation from this supersonic region is unable to travel upstream against the flow and go *outside* the horizon. Surfaces with  $z < z_H$  are said to form (acoustic) outer trapped surfaces and the outermost trapped surface is called the marginally outer trapped surface. If we think of a spherically symmetric static physical black hole, the marginally outer trapped surface coincides with the event horizon and the interior of the event horizon forms the trapped region containing outer trapped surfaces. (For a white hole, we would have similarly had inner trapped surfaces). The acoustic metric contains a time and position dependent overall conformal factor, but the location of the acoustic horizon as defined here does not depend on it.

### 3. UrQMD analysis for acoustic black hole horizon

#### *Search for local thermal equilibrium*

UrQMD (Ultra relativistic Quantum Molecular Dynamics) is a dynamical transport model based on an effective

solution of the relativistic Boltzmann equation used to describe the time evolution of a many-body system by using covariant equations of motion. The underlying degrees of freedom of UrQMD are hadrons (baryons, mesons and their antiparticles), their excited states, and resonances. UrQMD also includes string excitation and fragmentation (treated according to the LUND model [25, 26, 27]), formation and decay of hadronic resonances as well as rescattering of hadrons. We use UrQMD-3.3p2 model [19, 28, 29] to generate 5000 events at different times for Au-Au central collisions with laboratory energy of 10.7 GeV (BNL-AGS Experiment) [30, 31, 32, 33, 34, 35, 36, 37, 38]. (We have taken these parameter values for the collisions as sample values to demonstrate the possibility of acoustic black hole horizon and associated Hawking radiation in relativistic HIC.)

We start our analysis from time 6 fm (after the collision) by considering only nucleons, that is, protons and neutrons. In this work we do not include pions because then the resulting fluid would be better described by relativistic equations (though, as we have mentioned, still one can argue for the non-relativistic equations to be reasonable approximation for sub-sonic fluid velocities). As our formulation is based on non-relativistic fluid equations, it is much simpler to focus on a nucleon system which is genuinely a non-relativistic system at the temperatures considered. (Note that for nucleons, one has to be careful about the initial longitudinal velocities, which will not be part of the equilibrium distribution. We have taken care of that, as we will see below, by fitting Fermi-Dirac distributions at each value of  $z$  with a local fluid velocity which gives completely isotropic velocity distribution function.) A hydrodynamic description of the system is possible only after local thermodynamic equilibrium (LTE) has been attained. To check this, usually one takes a cubic or spherical cell around the centre of the system. We begin with a cubic cell of volume  $5 \times 5 \times 5 \text{ fm}^3$  centred around the centre of mass of the system located at  $z = 0$ . We follow the procedure of ref. [19] to check for equilibrium in this cell. First we need to verify whether the velocity distributions  $\frac{dN}{dv^\alpha}$  vs.  $v^\alpha$  obey Maxwell Boltzmann (MB) velocity distribution given by  $\frac{dN}{dv^\alpha} = e^{-m_N \frac{(v^\alpha)^2}{2T}}$  and overlap with each other. Here  $dN$  is the number of nucleons in the velocity bin  $dv^\alpha$  with  $v^\alpha$  denoting the velocity of individual nucleons in  $\alpha = x, y, z$  direction,  $m_N$  is the mass of a nucleon and  $T$  is the temperature of the cell. If these distributions overlap with each other, that is, if the momenta of the particles are isotropic, local thermal equilibrium is possible in this cell. We find that for our choice of cell dimension, a time of 6 fm is too short for achieving local thermal equilibrium. In this time, the transverse and longitudinal Maxwell Boltzmann velocity distributions do not overlap. In fact, the longitudinal velocity distribution does not even follow a Maxwell Boltzmann distribution at 6 fm time. Full equilibrium can be achieved in such a cell only around 13 fm time.

However, it is not necessary for the cell to be cubic or spherical and we find that when we take a rectangular cell with its longitudinal or  $z$  sides much smaller than the other two, we can get full equilibrium by 6 fm time. This is reasonable as the longitudinal velocity of particles has extra non-equilibrium contribution from the collision geometry, and this component becomes significant away from the centre of the collision in the longitudinal direction. In particular, when we take a cell of  $5 \times 5 \times 0.5 \text{ fm}^3$  at 6 fm time, the Maxwell Boltzmann velocity distributions of all velocity components are found to overlap<sup>2</sup>. The momentum spectrum of nucleons  $\frac{dN}{dp^\alpha}$  vs.  $E$ , with  $p^\alpha$  and  $E$  being the  $\alpha^{\text{th}}$  component of three momentum and energy of a nucleon respectively, follows a Fermi Dirac distribution,  $\frac{1}{\exp[(E-\mu_B)/T]+1}$ , and by fitting, we obtain the temperature of the cell to be  $\sim 154 \text{ MeV}$ . Here,  $\mu_B$  is the baryonic chemical potential. Note that here we are performing low energy collisions and taking the cell to be smaller in the  $z$  direction. So, baryon density and baryon chemical potential are significantly high, especially at 6 fm time. This makes quantum statistics significant. In fact, all three overlapping velocity distributions show some deviation near the tail from Maxwell Boltzmann velocity distribution. For longer times, Boltzmann distribution is good enough for fitting [19].

For hydrodynamic description of the system, local thermal equilibrium is required not only in the central cell, but in the off-centred cells as well. It is not guaranteed that off-centred regions would equilibrate at the same time as a central cell if we choose them to be of identical dimensions. By allowing the cell shape and size to vary with position, we are able to achieve local thermodynamic equilibrium simultaneously in a fairly large part of the system, thereby justifying a fluid description of the system.

#### *Locally static acoustic horizon in the plasma*

In the centre of mass frame, considering both the left and right half spaces, the longitudinal Maxwell Boltzmann velocity distribution of the particles,  $\frac{dN}{dv^z}$  vs.  $v^z$ , in an appropriately chosen cell at the origin, is symmetric about  $z = 0$  while the same in an off-centred cell is asymmetric about the value of  $z$  corresponding to the centre of that cell. If we do a Lorentz transformation in the  $z$  direction of longitudinal velocities of the particles such that the latter also becomes symmetric, we arrive at a frame comoving with the fluid at that specific value of  $z$ . This gives us the velocity of the fluid at that particular  $z$ , as measured in the centre of mass frame. We have performed calculation of plasma velocity for the region where  $z \geq 0$ . Due to symmetry of collision about  $z = 0$ , similar behaviour should hold for  $z \leq 0$  region also. In this way, we can find the velocity of the fluid at different points in the region  $0 < |z| < 5 \text{ fm}$  at different times. The result is plotted in figure 2 and shows the following features:

<sup>2</sup>For example, with a cell of volume  $5 \times 5 \times 2 \text{ fm}^3$ , local thermal equilibrium will be achieved at 7 fm time.

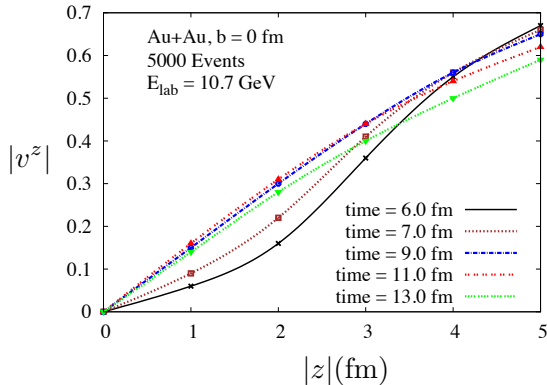


Figure 2: Longitudinal velocity of nucleonic fluid  $|v^z|$  (in units of speed of light,  $c$ ) vs.  $|z|$  at different times. Plot showing that acoustic horizon first moves towards the centre of the plasma, then remains fixed at  $|z| \approx 2.5$  fm for a time duration of 2 fm (9 – 11 fm), and then moves outward.

1. for  $0 < |z| < 4$  fm, the general behaviour is that at a fixed  $z$ ,  $|v^z|$  initially increases with time and then starts decreasing. The time at which this transition occurs depends on  $z$ , happening earlier at higher values of  $|z|$ ;
2. for  $4\text{fm} < |z| < 5\text{fm}$ ,  $|v^z|$  is monotonically decreasing.

This behaviour cannot be explained if we naïvely assume Bjorken expansion [39] for the plasma where  $v^z \sim z/t$  [39]. However, as we discussed above, for low energy collision with large nuclear stopping, Bjorken picture is not appropriate [39]. In our simulations, the centre of mass energy of the collision is low. This results in a narrow rapidity distribution which in turn gives rise to a strong pressure gradient along the  $z$  direction in the plasma. This pressure gradient accelerates the plasma in the region  $0 < |z| < 4$  fm but dies off near  $|z| = 4$  fm and beyond that, the longitudinal velocity at any fixed  $|z|$  decreases with time owing to expansion.

In ref. [19], the authors determine the equation of state for a hadronic system produced by the same collision occurring at the same energy as considered here, in the time interval 10 fm–18 fm to be  $p \simeq 0.12\epsilon$  in the central cell. Note, that the equation of state does not vary during this interval. Thus, the hadronic system has a constant speed of sound given by  $c_s = 0.35$  (in units of  $c$ ) in this period. If we assume that the same equation of state remains valid in the preceding time interval of 6 fm – 11 fm and is applicable to off-centred cells too, then an acoustic horizon is formed in the plasma at the position where

$$|v^z(t, z_H)| = 0.35. \quad (3)$$

Figure 2 reveals an interesting behaviour of this acoustic horizon - in the beginning, from time 0 fm – 9 fm, it moves towards lower values of  $|z|$ , then remains static at  $|z| \simeq 2.5$  fm for a duration of about 2 fm and again starts moving after  $t \approx 11$  fm, but now towards higher values of  $|z|$ . Even

if the speed of sound in the plasma has some other constant value, we would get a similar behaviour of the horizon as long as  $0 < c_s < 0.58$  (beyond this value, there is no time period over which one gets static horizon, in figure 2). Though, for low energy collision, it is improbable that  $c_s$  would reach 0.58. Of course, the associated time intervals in such situations would be different. However, if the speed of sound varied temporally and spatially, it would not be possible to predict the evolution of the horizon without explicitly knowing  $c_s(t, z)$ . On the other hand, if we had considered high energy collisions, like those occurring at RHIC and LHC, a strong pressure gradient would occur only for values of  $z$  corresponding to the decaying part of the rapidity distribution. In such situations, the speed of sound in the plasma would also increase to about 0.58. So, a similar evolution of the acoustic horizon could be expected.

#### 4. Surface gravity and Hawking temperature

In figure 2, the curves corresponding to  $t = 9$  fm and  $t = 11$  fm almost overlap upto  $|z| \approx 4$  fm. For  $c_s \approx 0.35$ , the acoustic horizon lies close to  $|z| \approx 2.5$  fm during this time interval. Remember that we have decided to look at the analogue spacetime emerging only in the plasma occupying the left half space (see figure 2). Regions of the acoustic spacetime with  $z < -2.5$  fm lie inside the acoustic black hole. Hawking radiation occurs from the part of spacetime lying just outside the horizon, but to experimentally identify signatures of this radiation, it may be necessary for us to probe the region lying inside the horizon too. Otherwise, from the point of view of a gravitational analogue, it is only the spacetime outside the horizon that is of concern to us. Now, an almost time independent profile of  $v^z$  in the interval 9 fm  $< t < 11$  fm for  $-4$  fm  $< z < 0$  offers us the great advantage of approximating the general dynamical metric of eq. (1) as a conformally static one given by:

$$g = \frac{\rho(t, z)}{c_s} \left[ - (c_s^2 - v^z(z)^2) dt \otimes dt + 2v^z(z) dt \otimes dz + dx \otimes dx + dy \otimes dy + dz \otimes dz \right] \quad (4)$$

$$= \Omega(t, z) \tilde{g} \quad (5)$$

where  $\Omega(t, z) = \frac{\rho(t, z)}{c_s}$  is a conformal factor depending on position in the acoustic spacetime. At first, we ignore the conformal factor. This brings us to a static acoustic metric  $\tilde{g}$  that is qualitatively similar to a static Schwarzschild metric written in Painlevé-Gullstrand coordinates with axial symmetry instead of spherical symmetry. It has a timelike Killing vector field  $\tilde{k}^a = (1, 0, 0, 0)$ <sup>3</sup>. This normalisation naturally gives

$$\tilde{g}(\tilde{k}, \tilde{k}) = -(c_s^2 - v^z(z)^2)$$

<sup>3</sup>All quantities defined in the spacetime with metric  $\tilde{g}$  will be distinguished by a tilde on top.

which gives  $\tilde{g}(\tilde{k}, \tilde{k}) = -c_s^2$  at  $z = 0$  ensuring that  $\tilde{k}$  matches with the four velocity of an observer in the asymptotically flat region of the acoustic spacetime (note the difference with general relativity where the speed of light is set to unity). The apparent horizon defined by  $c_s(z_H) = |v^z(z_H)|$  is also a Killing horizon for  $\tilde{k}$  since  $\tilde{g}(\tilde{k}, \tilde{k}) = 0$  on this surface. The surface gravity  $\tilde{\kappa}$  of a Killing horizon is defined by the relation

$$\nabla_a (\tilde{g}_{bc} \tilde{k}^b \tilde{k}^c) = -2\tilde{\kappa} \tilde{g}_{ab} \tilde{k}^b. \quad (6)$$

For the metric  $\tilde{g}$ , a simple calculation gives

$$\tilde{\kappa} = (c_s' - (v^z)')|_H$$

and as  $c_s$  is constant in our model, we simply have

$$\tilde{\kappa} = -(v^z)'|_H. \quad (7)$$

Since,  $(v^z)'|_H$  is negative,  $\tilde{\kappa}$  remains a positive quantity. Now, under the conformal transformation

$$\tilde{g}(t, z) \rightarrow g(t, z) = \Omega(t, z) \tilde{g}(t, z), \quad (8)$$

$\tilde{k}$  will remain a Killing vector field if

$$\tilde{k}(\Omega) = \tilde{k}^0 \partial_0 \Omega = 0. \quad (9)$$

Otherwise,  $\tilde{k}$  becomes a conformal Killing vector field and the Killing horizon a conformal Killing horizon:  $g(\tilde{k}, \tilde{k})|_H = \Omega|_H \tilde{g}(\tilde{k}, \tilde{k})|_H = 0$ . The definition of surface gravity by eq. (6) is conformally invariant even if  $\tilde{k}$  doesn't remain a true Killing vector field because, on the (conformal) Killing horizon,

$$\begin{aligned} \nabla_a (g_{bc} \tilde{k}^b \tilde{k}^c) &= \nabla_a (\Omega \tilde{g}_{bc} \tilde{k}^b \tilde{k}^c) \\ &= \tilde{g}_{bc} \tilde{k}^b \tilde{k}^c \nabla_a \Omega + \Omega \nabla_a (\tilde{g}_{bc} \tilde{k}^b \tilde{k}^c) \\ &= -2\Omega \tilde{\kappa} \tilde{g}_{ab} \tilde{k}^b \\ &= -2\tilde{\kappa} g_{ab} \tilde{k}^b. \end{aligned} \quad (10)$$

The first term in the second equality vanishes because on the Killing horizon  $\tilde{g}(\tilde{k}, \tilde{k}) = 0$ . However, for  $\tilde{\kappa}$  to be the surface gravity measured by an asymptotic observer in a spacetime with metric  $g$ , the normalisation of  $\tilde{k}$  has to be appropriately changed:  $k^a \rightarrow k^a = \frac{1}{\sqrt{\Omega(t,0)}} \tilde{k}^a$  such that

$$g(k, k)|_{z=0} = \Omega(t, 0) \tilde{g}(k, k)|_{z=0} = \tilde{g}(\tilde{k}, \tilde{k})|_{z=0} = -c_s^2. \quad (11)$$

The new surface gravity  $\kappa$  is obtained using the defining relation

$$\nabla_a (g_{bc} k^b k^c) = -2\kappa g_{ab} k^b. \quad (12)$$

This makes

$$\kappa = \frac{\tilde{\kappa}}{\sqrt{\Omega(t, 0)}} \quad (13)$$

and it is the surface gravity measured by an observer in the conformally flat asymptotic region of the acoustic spacetime with metric  $g$ . Such an observer sees a thermal spectrum of spontaneous radiation, the Hawking radiation, emanating from the (conformal) Killing horizon and when the corresponding (conformal) Killing vector field is normalised such that it matches with her four velocity in the asymptotic region (as done in eq. (11)), she finds that this radiation is at a temperature [40]

$$T = \frac{\kappa}{2\pi} = \frac{\tilde{\kappa}}{2\pi \sqrt{\Omega(t, 0)}} = \frac{\tilde{T}}{\sqrt{\Omega(t, 0)}}. \quad (14)$$

Here,  $\tilde{T}$  would have been the temperature measured by her if she were in the spacetime with metric  $\tilde{g}$ .

We now note that the acoustic metric in eq. (1) is derived starting from (non-relativistic) fluid equations that allow the freedom to multiply the metric by an overall constant. We utilize this to replace the conformal factor  $\Omega(t, z)$  in eq. (4) by  $\Omega(t, z)/\Omega(t_0, 0)$ . We take  $t_0$  to be some value in the time interval (9 – 11) fm relevant for our discussion in this section. Thus, in the asymptotically flat region, at  $z = 0$ , the new normalised conformal factor becomes unity at  $t = t_0$  and the temperature, as measured by the asymptotic observer, becomes

$$k_B T = -\frac{\hbar}{2\pi} (v^z)'|_H. \quad (15)$$

Here, we have restored the fundamental constants  $\hbar, k_B$  in the expression for Hawking temperature. Over the time period 9 fm  $< t < 11$  fm, the central density actually decreases. Asymptotic value of the conformal factor then does not remain 1, changing to  $\frac{\Omega(t, 0)}{\Omega(t_0, 0)} < 1$  for  $t > t_0$ . For 1-d expansion, central density decreases linearly, so for  $t_0 \sim 10$  fm, the change in density is about 20 % in a time duration of 2 fm ( $t \sim (9 - 11)$  fm). The proper time for the asymptotic observer is then changed by the factor  $\sqrt{\Omega(t, 0)/\Omega(t_0, 0)}$ , which is about 10% (for density change of order 20%). The temperatures measured by the asymptotic observer are then blue shifted by this amount. Thus, we conclude that the temperature observed by the asymptotic observer (at  $z = 0$ ) is given by eq. (15), with the value possibly increasing by about 10% due to decreasing central density. (Even though we have avoided consideration of dynamical horizon here, it is tempting to point out that for earlier time period ( $t < 9$  fm), the sonic horizon actually moves towards  $z = 0$ . One should then expect blue shifted Hawking radiation as observed by the asymptotic observer at  $z = 0$ .)

Before we discuss estimate of this temperature, it is instructive to derive this temperature using imaginary time formalism. For this we start with the following expression

for the acoustic metric in  $(\tau, x, y, z)$  coordinates:

$$ds^2 = \Omega(\tau, z) \left[ - (c_s^2 - v^z(\tau, z)^2) d\tau^2 + \left( \delta_{\alpha\beta} + \frac{v_\alpha v_\beta}{c_s^2 - v^2} \right) dx^\alpha dx^\beta \right]. \quad (16)$$

Here,  $v_\alpha = \delta_{\alpha\beta} v^\beta$ . This metric is related to the one in eq. (4) by a coordinate transformation from  $t \rightarrow \tau$  [3]:

$$d\tau = dt + \frac{\vec{v} \cdot d\vec{x}}{c_s^2 - v^2} \quad (17)$$

with velocity along  $z$ -axis. (Note that in the conformal factor, the density now depends on the new variable  $\tau$ .) We get,

$$ds^2 = \Omega(\tau, z) \left[ -c_s^2 d\tau^2 f(z) + \frac{dz^2}{f(z)} + dx^2 + dy^2 \right] \quad (18)$$

where

$$f(z) = 1 - \frac{v^z(z)^2}{c_s^2}. \quad (19)$$

For the near horizon geometry, we expand  $f(z)$  about  $z = z_H$  for  $z > z_H$ ,

$$f(z) = \left. \frac{\partial f(z)}{\partial z} \right|_{z_H} (z - z_H) \quad (20)$$

using  $f(z_H) = 0$  as  $v^z(z_H) = c_s$ . We now define a coordinate  $\rho_{sp}$  which is the proper distance from the horizon (subscript 'sp' is used to distinguish from the symbol  $\rho$  used for density):

$$d\rho_{sp} = \frac{dz}{\sqrt{f(z)}} = \frac{dz}{\sqrt{f'(z_H)} \sqrt{z - z_H}}. \quad (21)$$

Integration gives

$$\rho_{sp} = 2 \frac{\sqrt{z - z_H}}{\sqrt{f'(z_H)}}. \quad (22)$$

With this we can express  $f(z)$  as a function of  $\rho_{sp}$

$$f(z) = \frac{\rho_{sp}^2}{4} f'(z_H)^2 \equiv f(\rho_{sp}). \quad (23)$$

The near horizon metric then becomes

$$ds^2 = \Omega(\tau, z) \left[ -K^2 \rho_{sp}^2 d\tau^2 + d\rho_{sp}^2 + dx^2 + dy^2 \right], \quad (24)$$

where

$$K = \frac{f'(z_H) c_s}{2} = -(v^z)'(z_H), \quad (25)$$

as  $v^z(z_H) = c_s$ . Rest of the procedure is standard. We go to the Euclidean space with  $\tau \rightarrow -i\tau_E$ :

$$\begin{aligned} ds^2 &= \Omega(\tau, z) \left[ K^2 \rho_{sp}^2 d\tau_E^2 + d\rho_{sp}^2 + dx^2 + dy^2 \right] \\ &= \Omega(\tau, z) \left[ \rho_{sp}^2 d\theta^2 + d\rho_{sp}^2 + dx^2 + dy^2 \right], \end{aligned} \quad (26)$$

where  $\theta = K\tau_E$ . The two dimensional space spanned by  $(\rho_{sp}, \theta)$  has a conical singularity at  $\rho_{sp} = 0$  i.e. the location of the horizon, unless  $\theta$  is periodic with a period of  $2\pi$ . Since, there is no physical singularity at the horizon, we must have  $\theta \sim \theta + 2\pi$ . This implies that  $\tau_E$  is also periodic:

$$\tau_E \sim \tau_E + \frac{2\pi}{K}. \quad (27)$$

We thus conclude that the quantum fields in this space-time (which are fluctuations in the velocity potential) will be in thermal equilibrium with a temperature  $T$ ,

$$T = \frac{K}{2\pi} = -\frac{(v^z)'(z_H)}{2\pi} \quad (28)$$

which is the same as obtained earlier in eq. (15). The remaining argument is same as that following eq. (15). Suitably normalising by the factor  $1/\Omega(\tau_0, 0)$ , we conclude that the temperature observed by the asymptotic observer at  $(z = 0)$  is given by the above equation. (It is important to note that the conformal factor now depends on  $\tau$ , so the value  $\tau_0$  will correspond to  $t = t_0$  at  $z = 0$ .) Further, following the same argument about the effect of decrease in the central density on the conformal factor (as after eq. (15)), we conclude that the observed temperature may be larger by about 10% (when density decreases by about 20% for the relevant duration of time).

We now estimate the value of temperature. The relevant parts of the plots in figure 2 lie between  $|z| = 2 - 3$  fm. Recall that we had chosen to confine our attention to the region  $z < 0$ . The horizontal axis then should be read as negative values of  $z$ . To calculate  $(v^z)'(z_H)$  we use plots for  $t = 9$  and  $t = 11$  fm between  $z = -3$  and  $z = -2$  fm, as this encloses the value  $v^z(z_H) = c_s = 0.35$ . We get  $(v^z)'(z_H) \simeq 0.12 \text{ fm}^{-1}$ . The value of temperature is then

$$k_B T = \hbar \frac{(v^z)'(z_H)}{2\pi} \simeq \frac{0.12}{2\pi} \text{ fm}^{-1} \simeq 4 \text{ MeV}. \quad (29)$$

The temperature can increase by about 10 % due to decrease in central density by about 20% for the relevant time period. (We again mention that for  $t < 9$  fm, the sonic horizon actually moves towards the asymptotic observer at  $z = 0$ . From general physical consideration, one will expect higher value of the Hawking temperature due to the blue shift of the radiation.)

## 5. Observational prospects and conclusion

As the temperature of the plasma, even at low collision energies considered here, is about 135 MeV, it may be difficult to observe the signature of Hawking temperature of about 4-5 MeV. However, note that here the Hawking radiation will be from the region of acoustic horizon which will be away from the central region (where the plasma temperature is maximum). The expected temperature for large rapidity regions is smaller, which may help in identifying



the signal here. For observations, we recall that the temperature of the plasma at the freezeout surface depends on the longitudinal coordinate  $z$ , primarily due to  $z$  dependence of the chemical potential and also due to departure from strict Bjorken longitudinal boost scaling. Further, the longitudinal flow velocity of the plasma depends on  $z$  coordinate. Thus, hadrons coming out from a specific  $z$  value have specific rapidity contribution from this flow (called as frame rapidity) and also correspond to local  $z$  dependent temperature. This leads to well defined rapidity dependent particle distributions.

In the presence of Hawking radiation, this rapidity dependence of particle distributions will be changed. This is because the relevant scalar field here is the scalar perturbation over velocity potential,  $\psi$ , and hence, the Hawking radiation appears in the form of a thermal spectrum of excitations of  $\psi$ . Thus, at any value of  $z$  (between the collision centre and the acoustic black hole horizon) there will be a thermal distribution of perturbations in the velocity potential giving rise to a fluctuating component in flow velocity at that specific  $z$  value. Thus, the earlier  $z$  dependent flow velocity (in the absence of Hawking radiation) gets a fluctuating component. Also, the  $z$  dependence of temperature gets affected due to fluctuations in the local velocity. This directly affects the rapidity dependence of particle distributions. Specifically, say, rapidity dependence of transverse momentum  $p_T$  distributions of particles should have a thermal component. Thus, while fitting the observed rapidity dependence for these distributions, one should allow a thermal part in the rapidity distribution. We have not worked out the specific dependence yet coming from Hawking radiation, it requires detailed hydrodynamic simulations. We hope to present it in a future work. Our purpose in the present work has been to illustrate the basic physics of the phenomenon, and demonstrate its existence for our system under specific conditions.

For the present work, we have avoided the issue of dynamical horizon so that conceptual issues do not overshadow the main physics we want to illustrate, the possibility of observing Hawking radiation from acoustic black holes in heavy-ion collisions. Due to this limited focus, we have found a narrow window of time  $t$  of about 9 – 11 fm during which static horizon could be achieved. If freezeout happens much later, then this thermal component may get lost in subsequent thermalisation. In such a situation, one may be able to observe this signal in terms of thermal photons and di-leptons which come out of the QGP region without scattering. Rapidity dependence of distribution of these particles should then contain a hidden signal of a thermal stage for the rapidity variable, even for a short period of time.

As we discussed above, we restricted to low energy collisions because here static horizon could be achieved rather easily, even without considering possible variations in the sound velocity. As the Hawking temperature is related to the velocity gradient, for ultra-relativistic collisions, where

thermal equilibrium is reached very quickly (in times much less than 1 fm for LHC energies), the velocity gradient will be far larger, leading to large Hawking temperature. It is very unlikely to get static acoustic horizon in those cases, however, due to non-trivial energy density/pressure gradients, it may be possible to make the velocity of acoustic horizon much smaller than the sound velocity by suitable choices of nuclei and collision energies. With proper consideration of dynamical horizons then, a large Hawking temperature may be possible in those cases. Relevant fluid equations will then be relativistic hydrodynamics equations. Acoustic metric for relativistic hydrodynamics has been discussed in the literature [41, 42, 43], and we plan to discuss this very exciting possibility in future.

*Acknowledgment.* We are grateful to Amitabh Virmani, Sanatan Digal, Ananta P. Mishra, Ranjita K. Mohapatra, Yogesh Srivastava, Raghu Rangarajan, Nirupam Dutta and Rajiv V. Gavai for useful comments and discussions. We would like to specially thank Somnath De for introducing UrQMD to us. A part of the work done by AD is supported by the Polish National Science Center Grant No. 2018/30/E/ST2/00432. OG sincerely thanks Institute of Physics, Bhubaneswar for financial support and hospitality as this work was conceived and semi-completed during an extended visit there. We also thank an anonymous referee for a very careful checking of the paper and for making very important suggestions and corrections.

## Bibliography

## References

- [1] S. W. Hawking, Particle Creation by Black Holes, *Commun. Math. Phys.* 43 (1975) 199–220, [167(1975)]. doi:10.1007/BF02345020.
- [2] W. Unruh, Experimental black hole evaporation, *Phys.Rev.Lett.* 46 (1981) 1351–1353. doi:10.1103/PhysRevLett.46.1351.
- [3] M. Visser, Acoustic black holes: Horizons, ergospheres, and Hawking radiation, *Class.Quant.Grav.* 15 (1998) 1767–1791. arXiv:gr-qc/9712010, doi:10.1088/0264-9381/15/6/024.
- [4] C. Barcelo, S. Liberati, M. Visser, Analogue gravity, *Living Rev. Rel.* 8 (2005) 12, [Living Rev. Rel.14,3(2011)]. arXiv:gr-qc/0505065, doi:10.12942/lrr-2005-12.
- [5] M. Novello, M. Visser, G. Volovik (Eds.), *Artificial black holes*, River Edge, USA: World Scientific (2002) 391 p, 2002.
- [6] J. Steinhauer, Measuring the entanglement of analogue Hawking radiation by the density-density correlation function, *Phys. Rev. D* 92 (2) (2015) 024043. arXiv:1504.06583, doi:10.1103/PhysRevD.92.024043.
- [7] J. Steinhauer, Observation of thermal Hawking radiation and its entanglement in an analogue black hole, *Nature Phys.* 12 (2016) 959. arXiv:1510.00621, doi:10.1038/nphys3863.
- [8] J. R. Muñoz de Nova, K. Golubkov, V. I. Kolobov, J. Steinhauer, Observation of thermal Hawking radiation and its temperature in an analogue black hole, *Nature* 569 (7758) (2019) 688–691. arXiv:1809.00913, doi:10.1038/s41586-019-1241-0.
- [9] D. Kharzeev, K. Tuchin, From color glass condensate to quark gluon plasma through the event horizon, *Nucl. Phys. A* 753 (2005) 316–334. arXiv:hep-ph/0501234, doi:10.1016/j.nuclphysa.2005.03.001.

- [10] A. B. Nielsen, Black holes and black hole thermodynamics without event horizons, *Gen. Rel. Grav.* 41 (2009) 1539–1584. [arXiv:0809.3850](#), [doi:10.1007/s10714-008-0739-9](#).
- [11] P. Romatschke, U. Romatschke, Viscosity Information from Relativistic Nuclear Collisions: How Perfect is the Fluid Observed at RHIC?, *Phys. Rev. Lett.* 99 (2007) 172301. [arXiv:0706.1522](#), [doi:10.1103/PhysRevLett.99.172301](#).
- [12] O. Philipsen, The QCD equation of state from the lattice, *Prog. Part. Nucl. Phys.* 70 (2013) 55–107. [arXiv:1207.5999](#), [doi:10.1016/j.pnpnp.2012.09.003](#).
- [13] S. Borsanyi, G. Endrodi, Z. Fodor, A. Jakovac, S. D. Katz, S. Krieg, C. Ratti, K. K. Szabo, The QCD equation of state with dynamical quarks, *JHEP* 11 (2010) 077. [arXiv:1007.2580](#), [doi:10.1007/JHEP11\(2010\)077](#).
- [14] S. Borsanyi, G. Endrodi, Z. Fodor, S. D. Katz, S. Krieg, C. Ratti, K. K. Szabo, QCD equation of state at nonzero chemical potential: continuum results with physical quark masses at order  $\mu^2$ , *JHEP* 08 (2012) 053. [arXiv:1204.6710](#), [doi:10.1007/JHEP08\(2012\)053](#).
- [15] P. Parotto, M. Bluhm, D. Mroczek, M. Nahrgang, J. Noronha-Hostler, K. Rajagopal, C. Ratti, T. Schaefer, M. Stephanov, QCD equation of state matched to lattice data and exhibiting a critical point singularity, *Phys. Rev. C* 101 (3) (2020) 034901. [arXiv:1805.05249](#), [doi:10.1103/PhysRevC.101.034901](#).
- [16] A. Bazavov, et al., The QCD Equation of State to  $\mathcal{O}(\mu_B^6)$  from Lattice QCD, *Phys. Rev. D* 95 (5) (2017) 054504. [arXiv:1701.04325](#), [doi:10.1103/PhysRevD.95.054504](#).
- [17] J.-Y. Ollitrault, Relativistic hydrodynamics for heavy-ion collisions, *Eur. J. Phys.* 29 (2008) 275–302. [arXiv:0708.2433](#), [doi:10.1088/0143-0807/29/2/010](#).
- [18] D. Teaney, J. Lauret, E. V. Shuryak, Flow at the SPS and RHIC as a quark gluon plasma signature, *Phys. Rev. Lett.* 86 (2001) 4783–4786. [arXiv:nucl-th/0011058](#), [doi:10.1103/PhysRevLett.86.4783](#).
- [19] L. V. Bravina, et al., Local thermodynamical equilibration in central Au + Au collisions at AGS, *Phys. Lett. B* 434 (1998) 379–387. [arXiv:nucl-th/9804008](#), [doi:10.1016/S0370-2693\(98\)00624-8](#).
- [20] A. B. Nielsen, M. Visser, Production and decay of evolving horizons, *Class. Quant. Grav.* 23 (2006) 4637–4658. [arXiv:gr-qc/0510083](#), [doi:10.1088/0264-9381/23/14/006](#).
- [21] O. Ganguly, Acoustic Hawking radiation from evolving horizon in dynamical analogue spacetime (2019). [arXiv:1907.01905](#).
- [22] E. Bittencourt, V. A. De Lorenci, R. Klippert, L. S. Ruiz, Effective acoustic geometry for relativistic viscous fluids, *Phys. Rev. D* 98 (6) (2018) 064042. [arXiv:1807.05052](#), [doi:10.1103/PhysRevD.98.064042](#).
- [23] V. Mykhaylova, Shear viscosity to electrical conductivity ratio in the quasiparticle models, *Eur. Phys. J. ST* 229 (22-23) (2020) 3487–3496. [doi:10.1140/epjst/e2020-000116-9](#).
- [24] G. P. Kadam, H. Mishra, Dissipative properties of hot and dense hadronic matter in an excluded-volume hadron resonance gas model, *Phys. Rev. C* 92 (3) (2015) 035203. [arXiv:1506.04613](#), [doi:10.1103/PhysRevC.92.035203](#).
- [25] B. Andersson, G. Gustafson, B. Nilsson-Almqvist, A Model for Low p(t) Hadronic Reactions, with Generalizations to Hadron - Nucleus and Nucleus-Nucleus Collisions, *Nucl. Phys. B* 281 (1987) 289–309. [doi:10.1016/0550-3213\(87\)90257-4](#).
- [26] B. Nilsson-Almqvist, E. Stenlund, Interactions Between Hadrons and Nuclei: The Lund Monte Carlo, Fritiof Version 1.6, *Comput. Phys. Commun.* 43 (1987) 387. [doi:10.1016/0010-4655\(87\)90056-7](#).
- [27] T. Sjostrand, High-energy physics event generation with PYTHIA 5.7 and JETSET 7.4, *Comput. Phys. Commun.* 82 (1994) 74–90. [doi:10.1016/0010-4655\(94\)90132-5](#).
- [28] S. A. Bass, et al., Microscopic models for ultrarelativistic heavy ion collisions, *Prog. Part. Nucl. Phys.* 41 (1998) 255–369, [*Prog. Part. Nucl. Phys.* 41,225(1998)]. [arXiv:nucl-th/9803035](#), [doi:10.1016/S0146-6410\(98\)00058-1](#).
- [29] M. Bleicher, et al., Relativistic hadron hadron collisions in the ultrarelativistic quantum molecular dynamics model, *J. Phys. G* 25 (1999) 1859–1896. [arXiv:hep-ph/9909407](#), [doi:10.1088/0954-3899/25/9/308](#).
- [30] J. Barrette, et al., Directed flow and particle production in Au + Au collisions from experiment E877 at the AGS, *Nucl. Phys. A* 590 (1995) 259C–270C. [doi:10.1016/0375-9474\(95\)00240-2](#).
- [31] J. Barrette, et al., Proton and pion production relative to the reaction plane in Au + Au collisions at AGS energies, *Phys. Rev. C* 56 (1997) 3254–3264. [arXiv:nucl-ex/9707002](#), [doi:10.1103/PhysRevC.56.3254](#).
- [32] J. Barrette, et al., Directed flow of light nuclei in Au + Au collisions at AGS energies, *Phys. Rev. C* 59 (1999) 884–888. [arXiv:nucl-ex/9805006](#), [doi:10.1103/PhysRevC.59.884](#).
- [33] J. Barrette, et al., Directed flow of anti-protons in Au + Au collisions at AGS, *Phys. Lett. B* 485 (2000) 319–326. [arXiv:nucl-ex/0004002](#), [doi:10.1016/S0370-2693\(00\)00719-X](#).
- [34] H. Liu, et al., Sideward flow in Au + Au collisions between 2-A-GeV and 8-A-GeV, *Phys. Rev. Lett.* 84 (2000) 5488–5492. [arXiv:nucl-ex/0005005](#), [doi:10.1103/PhysRevLett.84.5488](#).
- [35] P. Chung, et al., Antiflow of K0(s) mesons in 6-A-GeV Au + Au collisions, *Phys. Rev. Lett.* 85 (2000) 940–943. [arXiv:nucl-ex/0101003](#), [doi:10.1103/PhysRevLett.85.940](#).
- [36] P. Chung, et al., Directed flow of Lambda hyperons in 2-AGeV to 6-AGeV Au+Au collisions, *Phys. Rev. Lett.* 86 (2001) 2533–2536. [arXiv:nucl-ex/0101002](#), [doi:10.1103/PhysRevLett.86.2533](#).
- [37] C. Pinkenburg, et al., Production and collective behavior of strange particles in Au + Au collisions at 2-AGeV - 8-AGeV, *Nucl. Phys. A* 698 (2002) 495–498. [arXiv:nucl-ex/0104025](#), [doi:10.1016/S0375-9474\(01\)01412-9](#).
- [38] C. Pinkenburg, et al., Production and collective behavior of strange particles in Au + Au collisions at 2-AGeV - 8-AGeV, *Nucl. Phys. A* 698 (2002) 495–498. [arXiv:nucl-ex/0104025](#), [doi:10.1016/S0375-9474\(01\)01412-9](#).
- [39] J. D. Bjorken, Highly Relativistic Nucleus-Nucleus Collisions: The Central Rapidity Region, *Phys. Rev. D* 27 (1983) 140–151. [doi:10.1103/PhysRevD.27.140](#).
- [40] A. B. Nielsen, J. T. Firouzjaee, Conformally rescaled spacetimes and Hawking radiation, *Gen. Rel. Grav.* 45 (2013) 1815–1838. [arXiv:1207.0064](#), [doi:10.1007/s10714-013-1560-7](#).
- [41] M. Visser, C. Molina-Paris, Acoustic geometry for general relativistic barotropic irrotational fluid flow, *New J. Phys.* 12 (2010) 095014. [arXiv:1001.1310](#), [doi:10.1088/1367-2630/12/9/095014](#).
- [42] N. Bilic, Relativistic acoustic geometry, *Class. Quant. Grav.* 16 (1999) 3953–3964. [arXiv:gr-qc/9908002](#), [doi:10.1088/0264-9381/16/12/312](#).
- [43] X.-H. Ge, S.-J. Sin, Acoustic black holes for relativistic fluids, *JHEP* 06 (2010) 087. [arXiv:1001.0371](#), [doi:10.1007/JHEP06\(2010\)087](#).